Journal of South American Earth Sciences 52 (2014) 108–118

Contents lists available at ScienceDirect

Journal of South American Earth Sciences

journal homepage: www.elsevier.com/locate/jsames

Seasonal patterns of rainfall and river isotopic chemistry in northern Amazonia (Guyana): From the headwater to the regional scale

Ryan Pereira [a,*], C. Isabella Bovolo [b,a], Nathan Forsythe [a], Nikolai Pedentchouk [c], Geoff Parkin [a], Thomas Wagner [a]

[a] School of Civil Engineering and Geosciences, Newcastle University, Newcastle upon Tyne, UK
[b] Iwokrama International Centre for Rainforest Conservation and Development, Guyana
[c] School of Environmental Sciences, University of East Anglia, Norwich, UK

ARTICLE INFO

Article history:
Received 24 June 2013
Accepted 11 February 2014

Keywords:
Climate
Guyana
Iwokrama
Hydrology
TRMM
ERA-Interim

ABSTRACT

We use first field-based observations of precipitation and river isotopic chemistry from a three-year study (2009–2011) in rainforest and nearby savannah in central Guyana at the northern rim of the Amazon rainforest to establish the quality of modelled or remotely-sensed datasets. Our 3 years of data capture a reduced rainfall regime in 2009 and an extended wet season in 2010, in contrast to the widely documented Amazonian floods in 2009 and droughts in 2010. Comparisons of observed precipitation with satellite derived TRMM and ECMWF ERA-Interim reanalysis precipitation show that both of these data sets capture the general pattern of seasonality, but substantially underestimate rainfall amounts in the primary wet season (by up to 50% and 72% respectively). The TRMM dataset is generally better at characterising the main dry season from September to December but the ERA-Interim model can overestimate precipitation in the dry season by up to 175%. Our new data on isotopic chemistry of river waters show that $\delta^2H/\delta^{18}O$ values in this region are broadly consistent with interpolated global datasets of modelled precipitation isotopic signatures. The dominance of isotopically lighter water derived from the rains of the ITCZ during the wet season provides evidence of the close coupling of water chemistry of headwater rivers on the northern rim of Amazonia to the positioning of the ITCZ over the region. Our results highlight the challenge in understanding and representing local scale hydrological and biogeochemical characteristics using regional scale model data. We argue that combining point and local scale field data with larger scale model data is necessary to progress towards a comprehensive understanding of climate–hydrology interactions in Amazonia.

1. Introduction

Amazonian tropical rainforests are important ecosystems for cycling water at local, regional and global scales (Eltahir and Bras, 1994). A number of studies have emphasised the increasing trend of extreme seasonal and inter-annual variability of precipitation and hydrology in the region, such as the severe floods and droughts in 2009–2010 in Amazonia (Lewis et al., 2011; Marengo et al., 2011; Tomasella et al., 2011), which were attributed to warming of the tropical North Atlantic (Booth et al., 2012) and subsequent anomalous southerly migration of the Inter Tropical Convergence Zone (ITCZ) (Marengo et al., 2012, 2011). The associated large variations in fluxes of water released from tropical rivers have been demonstrated, e.g. for the Amazon (Mayorga et al., 2005; Richey et al., 1990; Tomasella et al., 2011), Orinoco (Battin, 1998; Yamashita et al., 2010) and Essequibo (Pereira et al., 2014) rivers. These variations are associated with hydrochemical responses related to regional scale biogeochemical cycling (e.g. Richey et al., 2011; Tardy et al., 2005; for the Amazon; Laraque et al., 2013; for the Orinoco), which is an important component of the global carbon cycle.

Understanding of these regional tropical systems is currently hampered by poorly integrated monitoring networks (Martinez et al., 2013). Remote sensing technologies combined with global models can provide suitable data to characterise the climatic controls on large scale river dynamics. However, large uncertainties remain in understanding climate dynamics and variability in Amazonia. This lack of knowledge is mainly because of the uneven coverage of field study sites, which do not provide an adequate representation of larger areas (Batistella et al., 2009). Logistical and

* Corresponding author.
E-mail address: ryan.pereira@ncl.ac.uk (R. Pereira).

http://dx.doi.org/10.1016/j.jsames.2014.02.005

other constraints in remote tropical rainforests commonly result in localized, widely scattered datasets, requiring interpolation or upscaling to understand regional patterns, often based on few ground-based datasets.

In comparison with the central Amazon rainforest, the climate and hydrology of the northern Amazonia rainforests of the Guiana Shield region (incorporating Guyana, Suriname, and French Guiana, collectively known as 'the Guianas', with parts of southern Venezuela and northern Brazil) are even less well known. This region however, has one of the lowest deforestation rates, and incorporates approximately 15% of the forest in South America (Hammond, 2005). As deforestation trends continue elsewhere, the Guiana Shield will increasingly represent a greater share of the remaining intact forest cover (Hammond, 2005), and may provide a crucial link in maintaining moisture transfer from the Caribbean into central Amazonia (Marengo, 2009). There is also uncertainty in the regional climate understanding, reflected by lack of consensus in Global Climate Model future scenarios for the equatorial South American region, and in the Guiana Shield region in particular (e.g. McSweeney et al., 2010), emphasising the need for more small-scale studies that link local processes with larger climate dynamics.

Observation based interpolated climate datasets of the region do not allow an accurate representation of the climate of this area, because they incorporate few, if any records from Guyana (e.g. NOAA Climate Prediction Centre unified gauge-based analysis of global daily precipitation datasets for 1970–2005 (http://www.cpc.ncep.noaa.gov/products/precip/realtime/GIS/SA/SA-precip.shtml, see also Chen et al. (2008)). Other datasets cover only the Amazon or Brazil (e.g. Shi et al., 2000; Silva et al., 2007), thereby missing the Guiana Shield area altogether. Global datasets (e.g. CMAP, Xie and Arkin, 1997; GPCP, Adler et al., 2003) combine similar sets of limited observations with satellite or model outputs only at a coarse grid-scale (2.5° × 2.5° latitude–longitude grids).

A recent study of the precipitation and temperature regimes of the Guianas (Bovolo et al., 2012) has shown that reanalysis datasets (specifically ECMWF ERA-40, with a 1.125° grid) provide a reasonably good representation of monthly, annual and averaged seasonal temperature across the region when compared with observations. However, the reanalysis data is limited in representing precipitation amounts (Bovolo et al., 2012). The newer ECMWF ERA-Interim dataset offers a better representation of the water cycle due to revisions in the humidity analysis and bias correction for radiance data (Dee et al., 2011) at an increased 0.75° resolution. In a comparison of descriptions of the hydro-climatology of the Amazon basin between ERA-Interim and ERA-40 data and local observations, Betts et al. (2009) found that ERA-Interim remedied substantial drawbacks in the ERA-40 precipitation climatology of the Amazon basin but still suffered from a general dry bias, specifically in the amplitude of the seasonal precipitation cycle, in comparison with local observations. A better spatial resolution is achieved by TRMM (Tropical Rainfall Measuring Mission) satellite observations (grid scale of 0.25°). However, there are uncertainties in the TRMM rainfall anomaly algorithms to predict rainfall (Clarke et al., 2011; Li et al., 2012). TRMM data have been used in Amazonia (Collischonn et al., 2008), but no published studies have yet assessed or used TRMM data in the Guiana Shield region.

The δ^2H and δ^{18}O isotopic composition of precipitation and inland waters have been applied successfully to understand spatial and temporal patterns of hydrology (Araguas-Araguas et al., 2000; Bohnke et al., 2002; Clark and Fritz, 1997; Craig, 1961; Dansgaard, 1964; Dawson and Simonin, 2011; Fricke and O'Neil, 1999; Gat, 2004; Martinelli et al., 1996; Matsui et al., 1983; Rozanski et al., 1993). In northern Amazonia and the Guianas, the degree of depletion of δ^2H and δ^{18}O isotopes in precipitation has been attributed to the seasonal displacement of the ITCZ that controls the movement of moist air masses (Bowen and Revenaugh, 2003; Feng et al., 2009; Vuille et al., 2003). Stable water isotopes of inland waters have also been used successfully to determine water sources, assess the contribution of overland- and base-flows to stream flow, and establish potential rates of evaporation (Martinelli et al., 1996; Saylor et al., 2009; Speed et al., 2011; Strauch et al., 2006; Wassenaar et al., 2011). However, there are few observational data available for this region in the International Atomic Energy Agency-Global Network of Isotopes in Precipitation or Rivers (IAEA-GNIP/GNIR) databases, and most of the available records are very short (Vuille et al., 2003). To compensate for the lack of field-based data in the tropics, various interpolation models have been developed and used to identify monsoonal, altitudinal and seasonal dynamics (Bowen and Revenaugh, 2003; Gonfiantini et al., 2001; Saylor et al., 2009; Sturm et al., 2007; Vuille et al., 2003; Vuille and Werner, 2005), and impacts from deforestation (Bowen et al., 2005; Henderson-Sellers et al., 2002). However, the underlying processes and feedbacks that control regional hydro-climate dynamics of this region are not well constrained.

This study presents first precipitation, hydrology and isotopic chemistry results from 2009 to 2011 for rainforest and the neighbouring forest-savannah transition zone in central Guyana, which represent part of a wider frontier forest that extends approximately 500 km from southern Venezuela to the Guyanese-Brazilian border in the south (Fig. 1). These results help to address the paucity of field observations in this region, and are compared with data from global models of precipitation and isotopic chemistry to assess whether these models may be used in studies related to

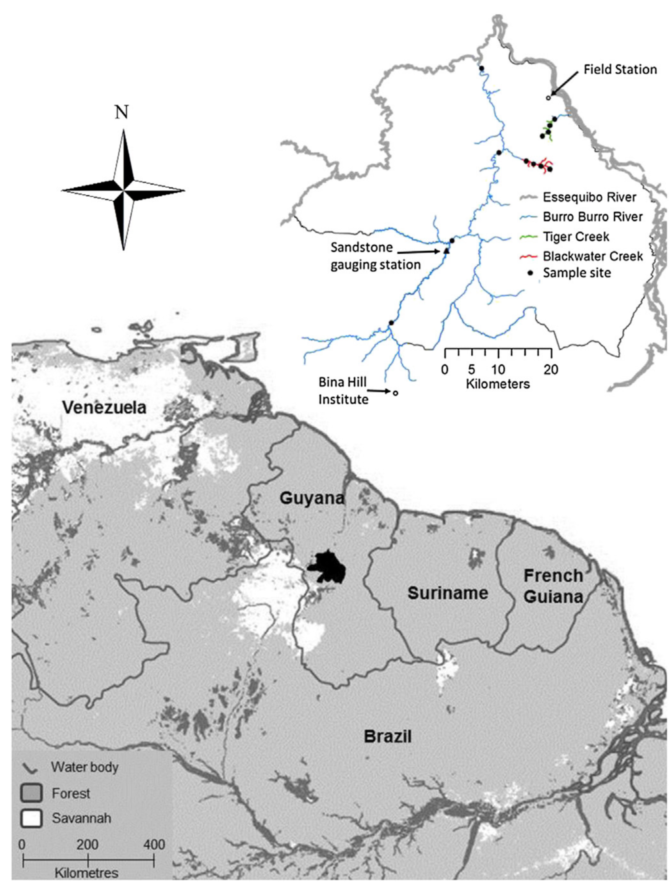

Fig. 1. Forest coverage of the Guiana Shield (after Gond et al., 2011) with inset of Iwokrama and relevant tributaries of the Burro Burro river catchment and focus catchments. (For interpretation of the references to colour in this figure legend, the reader is referred to the web version of this article.)

hydrological cycles in regional scale river systems fed by the Guyana Shield (e.g. Laraque et al., 2013).

2. Material and methods

The Iwokrama rainforest in central Guyana comprises 371,000 ha (Fig. 1) and is bounded by the Essequibo River to the East and the Siparuni River, a tributary of the Essequibo, to the west and north (Fig. 1). It lies just north of the Rupununi savannah wetlands. Iwokrama is situated near the northern extent of the Inter-Tropical Convergence Zone (ITCZ), where there is a transition in the climate regime from north (coastal) to south (savannah) from two wet seasons (primary: May–July and secondary: December–January) and two dry seasons (primary: centred around October and secondary: centred around March) to one wet season (May–August) and one long dry season (September–March) (Bovolo et al., 2012).

The Burro Burro catchment, a tributary of the Essequibo river (the 29th largest river by flow rate in the world (Dai and Trenberth, 2002), covers some 3200 km^2 (Hawkes and Wall, 1993) with approximately 2020 km^2 situated within the Iwokrama Reserve. The main channel of the Burro Burro River bisects the Iwokrama forest, flowing northward from the southern boundary of the forest–savannah transition, forming an approximate 65 km riverine transect. The topography of the catchment ranges from 52 to 995 m above sea level and incorporates a combination of low-lying undulating plains and steeper ranges of the Pakatau hills and the Iwokrama and Turtle mountains (Hawkes and Wall, 1993). Within the Iwokrama rainforest, two small-scale, lowland headwater catchments were studied; each approximately 5–6 km in length with an estimated catchment area of about 15–20 km^2. These 'focus' catchments are located adjacent to each other, and discharge into the Burro Burro River (Blackwater Creek) and directly into the Essequibo River (Tiger Creek). Both focus catchments are situated on similar acid-intermediate volcanic geology, overlain with highly-leached, quartzite, brown and white sands and an approximate 100 mm humic surface layer, with similar forest types including Greenheart (*Chlorocardium rodiei*), Black Kakaralli (*Eschweilera subglandulosa*) and Wamara (*Swartzia leiocalycina*).

One notable difference between the catchments is that the Tiger Creek catchment was harvested for commercial timber species from 2007 to 2009 using reduced impact-logging (RIL) techniques, removing approximately 400 trees. When compared with conventional clear-fell logging techniques, the impact of RIL upon a forest ecosystem is significantly mitigated by reducing the number of trees damaged during logging and aiding ecosystem recovery rates (Macpherson et al., 2012, 2010; Miller et al., 2011; Pinard and Putz, 1996).

2.1. Installation

A new hydro-climate and geochemistry monitoring programme was established in March 2010. Here, we present results from new equipment, together with some pre-existing storage raingauges. A new automatic weather station (AWS; Casella CEL, Bedford, United Kingdom) was installed within the Iwokrama forest approximately 80 km from the rainforest-savannah boundary. This complements a pre-existing manual storage rain gauge (127 mm diameter) in the savannah lands of Annai to form a north-south meteorological transect monitoring the precipitation patterns across a strong change in forest and savannah biomes (Fig. 1). Prior to March 2010, total daily rainfall was recorded at Iwokrama Field Station using a standard manual storage rain gauge (127 mm diameter). Where daily rainfall was not recorded (either manually or by the AWS), daily totals were estimated using accumulated measurements from the storage rain gauge.

The two focus catchments were instrumented for stage using DCL 9500 Level Sensors (Gems) calibrated to manual stage board readings. The sensors were housed within a stilling well and connected through a vented cable to a Frog RX data logger (Isodaq Technology). Flows were measured periodically across the range of observed conditions using a StreamPRO ADCP (Acoustic Doppler Current Profiler; Teledyne RD Instruments) at Blackwater Creek, and a Braystoke current meter (Valeport) at Tiger Creek. Rating curves were constructed using these data, and used to convert the monitored stage into flow records for each focus catchment.

2.2. Sampling and analysis for river geochemistry

To complement the hydro-climate monitoring programme, river water was collected from the main channel of the Burro Burro during the dry and wet seasons (March and July) of 2010 at four instream locations (04°46.965, 58°51.018; 04°34.217, 58°49.049; 04°16.563, 59°00.036; and 04°11.114, 59°03.758) forming a north-south transect (Fig. 1). The focus catchments were sampled from the centre of the river channel during the same dry and wet seasons of 2010 and again in 2011 (March and June/July in each year) from the river source at three locations approximately 1.5 kms apart (Blackwater Creek 04°32.968, 58°46.401; 04°32.747, 58°45.541; 04°32.821. 58°45.402; 04°32.744, 58°45.393 and Tiger Creek 04°36.521, 58°43.261; 04°36.188, 58°43.030; 04°36.024, 58°43.001; 04°36.201, 58°42.918). In total, four samples were collected from each focus catchment during each season. Sampling dates were: Blackwater Creek on 05/03/2010, 29/07/2010, 25/03/2011, 23/06/2011; Tiger Creek on 03/03/2010, 17/07/2010, 26/03/2011, 22/06/2011; and Burro Burro River on 20–22/03/2010, 10–12/07/2011. All samples were field filtered using Pall Acrodisc 0.45 μm filters, cold stored in Nalgene bottles and shipped to the UK for analysis. Water samples were analysed for oxygen and hydrogen isotopes. Water samples were analysed for oxygen and hydrogen isotopes ($\delta^2H/\delta^{18}O$) using a Picarro Cavity Ring-Down Spectroscopy (CRDS) analyser in the School of Chemistry and Pharmacy at the University of East Anglia, Norwich, UK. Three calibration standards, USGS W64444, GISP, and USGS W67400, were run at the beginning and at the end of each sequence of samples. Sample results were calibrated to these standards using linear least squares regression. A laboratory standard NTW (Norwich Tap Water) was measured along with the standards to monitor reproducibility of the results. Each sample was measured 6 times and the first three measurements discarded to account for memory effect. The precision of sample δ^2H and $\delta^{18}O$ measurements was better than 1.2 and 0.3‰, respectively.

2.3. Modelled precipitation

Reanalysis datasets offer physically coherent and realistic atmospheric parameters representing available historical observations at a global scale. The ECMWF ERA-Interim reanalysis is derived from modified operational weather forecast and analysis models, run in a retrospective manner (Dee et al., 2011). The precipitation outputs come as a forecast product from a 12-h analysis cycle, where available observations are combined with prior information from the forecast model to estimate the evolving state of the global atmosphere and at the earth's surface. Although not directly observed, precipitation is constrained by the temperature and humidity information derived from the assimilated observations used to initialise the forecast. ERA-Interim daily precipitation time series data were downloaded from the ECMWF data server for the period 1st Jan 1979–31st Dec 2011 (http://data-portal.ecmwf.int/data/d/interim_full_daily) and the two grid cells encompassing the observation area covered by the field based studies were extracted (Fig. 2).

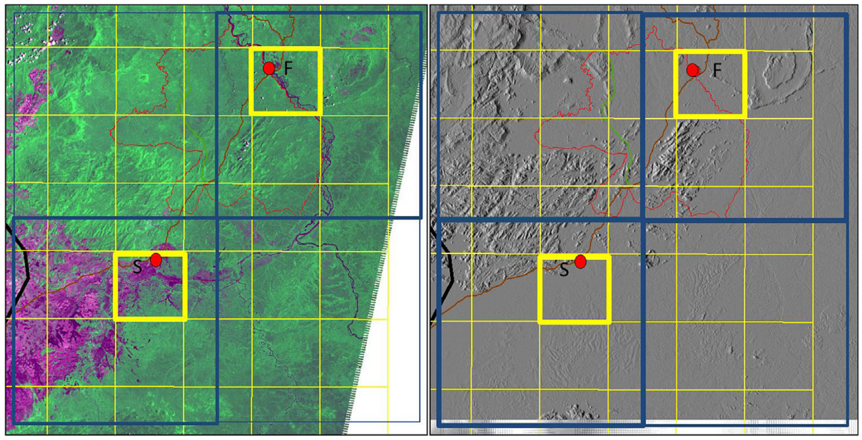

Fig. 2. (Left) Landsat image (derived from http://earthexplorer.usgs.gov/) showing forest vegetation in green and savannah in pink and (right) USGS Earth Explorer GLS-2005 30 m resolution digital elevation model map showing relief (downloaded June 2009 from http://edcsns17.cr.usgs/gov/EarthExplorer) overlaid by TRMM grid cells (yellow) and ERA-Interim grid cells (blue). Forest and savannah rain gauges raingauges are labelled F and S respectively. Selected TRMM and ERA-Interim grid-cells are highlighted in bold. (For interpretation of the references to colour in this figure legend, the reader is referred to the web version of this article.)

Satellite observations offer the possibility of improved spatial and temporal resolution global estimates of precipitation by direct observation. The TRMM satellite includes precipitation radar, a microwave imager and the Visible and Infrared Radiometer sensors (Huffman et al., 2007). The TRMM multi-satellite precipitation analysis (TMPA) uses combinations of satellite sensors and, where possible, land-surface precipitation gauge analyses in an attempt to improve accuracy, coverage and resolution of satellite based observations and outputs data on a 0.25 × 0.25° spatial resolution in a global belt extending from 50°S to 50°N latitude (Huffman et al., 2007). Algorithm 3B42 produces merged high quality/infrared precipitation and root-mean-square precipitation error estimates on a 3-h temporal resolution (http://trmm.gsfc.nasa.gov/3b42.html). It combines microwave estimates of precipitation with infrared precipitation estimates calibrated using the microwave precipitation, which are then rescaled to monthly resolution. TRMM version 7a represents a minor correction to TRMM v7. This change is not methodological in nature, but rather corrects for omission of one specific source of microwave data in the original processing of the v7 outputs. TRMM 3b43 v7a monthly gauge adjusted satellite estimates from 1st Jan 2009 to 31st Dec 2011 were extracted from http://reverb.echo.nasa.gov for the two grid cells encompassing the available observations (Fig. 2).

2.4. δ^2H and δ^{18}O precipitation maps

Spatial variability in the δ^2H and δ^{18}O of precipitation reflects the combination of rainout effects and recycling effects within air masses bringing water vapour to different geographic regions. The largest database of precipitation δ^2H and δ^{18}O is stored on the Water Isotope System for Data Analysis, Visualization, and Electronic Retrieval (WISER) at http://www-naweb.iaea.org/napc/ih/IHS_resources_isohis.html. This dataset has been used to produce mean monthly δ^2H and δ^{18}O of precipitation maps for the globe (Bowen et al., 2005). Mean monthly δ^2H and δ^{18}O precipitation maps were downloaded from http://wateriso.eas.purdue.edu/waterisotopes for the grid cell that covers the Burro Burro catchment.

3. Results

3.1. Observed precipitation

Monthly rainfall totals from January 2009 to December 2011 (Table 1) in the forest, generally demonstrate a strong primary wet season from May to August in the forest and primary dry season beginning at the end of September (100 mm/month used as the indicator of a dry season, after Sombroek (2001)). Although a secondary wet-season in November is common on coastal regions (Bovolo et al., 2012), our data for the rainforest shows only small increases in rainfall during this period, but with very wet March months in both 2009 and 2011. A short secondary dry season was observed in April 2009 and 2011 before the primary wet season. In 2009, the primary wet season was shorter with less rainfall in May than 2010 and 2011. Annual rainfall totals (2101, 3342 and 2646 mm for 2009, 2010 and 2011, respectively) show that 2009 was relatively drier, than 2010 and 2011. This precipitation pattern is in contrast to the intense, longer than normal rainy season recorded in the northern and north-western Amazon basin in 2009, which caused extreme flooding (Marengo et al., 2012) and the drought in central Amazonia in 2010 (Lewis et al., 2011; Marengo et al., 2011).

The overall seasonal weather pattern in the savannah, less than 10 km from the rainforest-savannah boundary (Table 1) was comparable to the forest with the primary wet season occurring from May to June and the primary dry season beginning in October. However, the savannah did not receive pronounced wet March months in 2009 and 2011, although the ‘secondary wet-season’ centred in November is still recognisable. Annual rainfall totals (1849, 3318, 2730 mm over 2009, 2010 and 2011 respectively) in the savannah show that it was much drier than the rainforest in 2009 and was classed locally as a drought, whilst 2010 was much wetter than 2009 with severe flooding.

3.2. Modelled precipitation

Tropical rainforests experience high amounts of convective rainstorms which can lead to high spatial variability. Therefore comparisons of point rain-gauge observations with modelled grid cells, which are representative of an averaged area, are not likely to give good results unless the rain gauge location is representative of conditions over a wider area. To assess the spatial representation of the new AWS dataset, a comparison was made against a tipping-bucket raingauge at a similar elevation, located within the forest approximately 9 km away. The datasets show that although precipitation between gauges vary spatially on a daily timescale, rainfall over a monthly timescale is similar at both locations ($R^2 = 0.88$ based on a 17 month time-series between 2010 and 2012). Total rainfall recorded in the rainforest over these 17 months

Table 1
Total monthly observed rainfall, estimates from TRMM and ERA-Interim models from the forest and savannah and monthly averaged river discharge for Tiger and Blackwater Creek.

	Forest-Iwokrama field station (mm)			Savannah-Annai (mm)			River discharge (m^3/S)	
	Observed	TRMM	ERA-interim	Observed	TRMM	ERA-interim	TC	BC
Jan-2009	199.7^{+}	147.4	217.2	176.2	192.9	111.8	–	–
Feb-2009	160.4^{+}	95.6	113	35.3	53.9	43	–	–
Mar-2009	423.5^{+}	42.9	124.5	77.3	31.6	46.7	–	–
Apr-2009	79.0^{+}	174.7	145.1	92.5	85.5	60.2	–	–
May-2009	72.9^{+}	139.8	44.3	60.7	85.3	17.3	–	–
Jun-2009	316.1^{+}	299.8	215.7	315.8	290.9	169.7	–	–
Jul-2009	411.1^{+}	307.7	218.8	421	368.2	208.7	–	–
Aug-2009	121.5^{+A}	122.4	165	214.2	111.7	166.2	–	–
Sep-2009	38.5^{+}	101.1	80.6	113.2	29.1	62.4	–	–
Oct-2009	121.2^{+}	62.1	116	71.1	81.5	62.6	–	–
Nov-2009	43.1^{+A}	35.1	118.5	107	36.2	67.3	–	–
Dec-2009	114.3^{+A}	134.3	129.1	155.4	104.1	48.6	–	–
Jan-2010	116.4^{+A}	95.7	71.8	95.5	33.8	16.3	–	–
Feb-2010	82.5^{+A}	35.5	57.3	86.3	85.2	22.4	–	–
Mar-2010	128.0^{M+A}	59.3	111.6	124	63.7	49.1	0.02^{M}	0.29^{M}
Apr-2010	412.4	232.6	192.2	425.3	189.9	155.9	0.08	1.57
May-2010	684.8	390.4	305.1	477.7	338	280.5	0.23	2.30
Jun-2010	494.2	322.4	273.0	524.7	299	237.5	0.30	2.92
Jul-2010	450.4^{MA}	345.4	292.7	387.3	418.2	259.7	0.47^{M}	4.45^{M}
Aug-2010	368.8^{MA}	388.1	231.4	500.2	293.3	244.8	0.25^{M}	–
Sep-2010	178	85.3	172.4	267.4	104.3	149.8	0.21	0.85^{M}
Oct-2010	112	50.3	118.6	61.7	39.9	104.1	0.11	0.35^{M}
Nov-2010	162.0^{M}	149.2	175.6	197.3	81.7	131.7	0.08	0.51^{M}
Dec-2010	152.7^{M}	194.1	152.2	170.4	103.9	91.7	0.13^{M}	0.67
Jan-2011	123.8	84.2	93.4	118.1	50.5	50.3	0.08^{M}	0.41
Feb-2011	185.5	259	127.6	62.1	77.3	56.5	0.10^{M}	0.95
Mar-2011	312	394	177.5	247.2	173.1	91	0.20	1.04^{M}
Apr-2011	111.5	53.2	73.3	75.8	24.5	32.5	0.13	0.72^{M}
May-2011	661.5	496.5	315.7	480.3	454.9	306.4	0.54	3.94^{M}
Jun-2011	312	363.7	288.3	691.9	352.7	285.1	0.37	4.15^{M}
Jul-2011	318	297.3	255.0	479.9	242.6	232.2	0.31	1.91^{M}
Aug-2011	144	161	197.2	278.8	200.5	166.5	–	–
Sep-2011	100.5	87.4	176.6	127	87.5	180.4	–	–
Oct-2011	149	138.1	169.8	119.5	89	149.1	–	–
Nov-2011	112	88.7	174.1	39.1	70.8	138.3	–	–
Dec-2011	116.5	138.6	125.6	10.1	18.8	67.7	–	–

^{M}missing data in month, $^{+}$ storage rain gauge measurement, ^{A}approximated with tipping bucket and storage gauges.

was 5034 mm compared with 5991 mm at the raingauge 9 km away, representing a difference of approx. 17% (note that one month was responsible for 532 mm difference in one month). At the larger grid-scale used by ERA-Interim, there is little variation in relief or land cover (thick blue box in Fig. 2). However, there are some relatively small mountain ranges with elevations from 80 to 800 m that exist south of the AWS raingauge which make the average relief of the ERA-Interim grid cell slightly higher than at the raingauge location. This may cause modelled precipitation to appear slightly higher than actually observed due to orographic forcing.

In the savannah, comparison of our manual storage raingauge with a tipping bucket raingauge located approximately 3 km away gives a correlation coefficient of 0.85 from 18 months of data between 2010 and 2011, with total rainfall of 4131 and 4948 mm respectively, a difference of approx. 18%. The slightly lower correlation is attributed to differences in the collection methods (i.e. manual vs. tipping bucket) and to the use of accumulated precipitation values over certain days in the manual time-series, which may have errors from evaporative losses. As seen in Fig. 2, the 'savannah' raingauge is near several small 'forest-islands' and is partly surrounded by the rainforest-savannah boundary, which extends around the area. The raingauge therefore characterises land cover of approximately 50% savannah and 50% rainforest which is comparable to the larger areas represented by the TRMM and the ERA-Interim grid cells. In terms of elevation, the area south of the raingauge has low relief and low elevation and we therefore assume that the raingauge location is representative of the TRMM grid cell. To the north of the raingauge, there are some small mountainous areas that suggest the ERA-Interim grid cell has a higher average elevation than at the raingauge location. It would therefore be expected that the ERA-Interim dataset may slightly overestimate rainfall in this grid-cell. Changing of the prevailing winds from the north-east, east or south-east, depending on the location of the ITCZ (Bovolo et al., 2012), may also cause a rain shadow of the grid-cell but these local effects should be captured by the raingauge.

The TRMM and ERA-Interim data capture a similar precipitation pattern to the observed 2009–2011 data sets with increased precipitation from May to August associated with the primary wet season. However, both models significantly underestimate the precipitation recorded at the forest and savannah sites, especially in the primary wet season; and the ERA-Interim overestimates rainfall slightly in the secondary wet season (Fig. 3). In the primary wet season of the 2009 'dry' year, TRMM underestimates observed rainfall by 5–25% for the rainforest and 8–48% in the savannah. In the 2010 and 2011 'wet' years this discrepancy is more pronounced, with rainfall underestimated by 7–43%, and 5–50% in the rainforest and savannah, respectively. ERA-Interim fares worse, underestimating rainfall in the primary wet season by 22–72%, 33–55% and 8–59% in 2009, 2010 and 2011, respectively. Both datasets also overestimate precipitation in the dry season from September to December but the ERA-Interim dataset is most pronounced overestimating observed precipitation by 6–175%. In total, over the 3 years, ERA-Interim rainfall underestimates rainfall by 53% in the

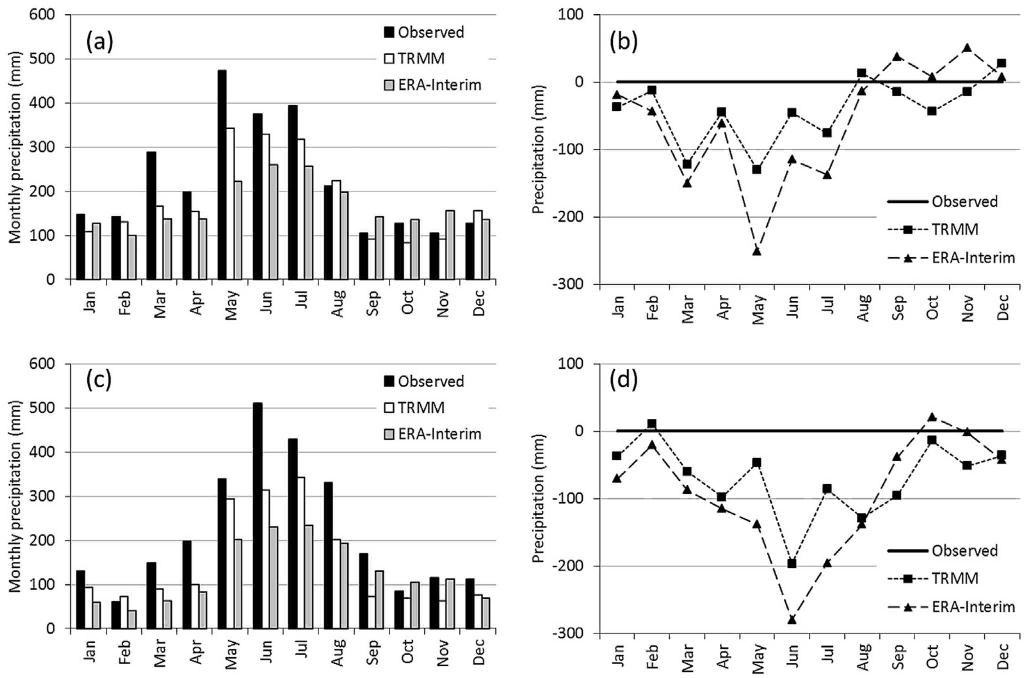

Fig. 3. Comparison of measured monthly precipitation averaged over 2009–2011 against TRMM and ERA-Interim datasets for the forest (a and b) and savannah (c and d). Plots a and c display recorded values. Plots b and d show the difference between the observed and modelled data.

forest and 58% in the savannah, whilst TRMM underestimates rainfall by 43% in the forest and 56% in the savannah.

3.3. *River hydrology*

Daily averaged river discharges for Blackwater and Tiger Creek are presented in Table 1, providing the context for river geochemical sampling within the seasonal rainfall pattern. A near complete time series record for Tiger Creek exists from the end of March 2010 to December 2011 with gaps from the end of July to the end of August 2010 and the end of December 2010 to mid-February 2011, due to instrument failures. Continuous records for Blackwater Creek are only available from end of March to end of July 2010 and end of November 2010 to mid-March 2011, again due to instrument malfunction. Blackwater Creek has a higher and flashier flow than Tiger Creek, with discharges ranging from 1 to 8 m^3/s, whereas Tiger Creek discharges rarely reach over 1 m^3/s.

3.4. *River geochemistry*

Water isotope analyses were conducted on 40 river water samples (Table 2). The δ^2H and δ^{18}O values are plotted in Fig. 4a with the Global Meteoric Water Line (GMWL), which represents the global average relationship between δ^2H and δ^{18}O in terrestrial waters across a latitudinal gradient (GMWL, Craig, 1961; Rozanski et al., 1993). Rainwater that has a deuterium excess can be indicative of either, effects of 'rainout' from orographic and convective rainfall, the 'amount effect' from increased rainfall or distance from the coast (Dansgaard, 1964). The overall ranges of the δ^2H and δ^{18}O values are −47 to −5.9‰ and −7.6 to −2.1‰, respectively. Generally, the dataset plots along or near the GMWL with a correlation coefficient of 0.99 and a slope of 7.33 (see Fig. 5).

The Burro Burro River water displays a change in isotopic signature from March (very dry) to July (wet month following a very wet period) during 2010. March samples display isotopic ranges of δ^2H from −12.4 to −9.3‰ and δ^{18}O of −3.0 to −2.5‰. In

Table 2
Water isotope values (δ^2H and δ^{18}O) of river water collected during dry and wet seasons in 2010 and 2011.

Sample site	March 2010		July 2010		March 2011		June 2011	
	Dry season		Wet season		Dry season		Wet season	
	δ^{18}O (‰)	δ^2H (‰)	δ^{18}O (‰)	δ^2H (‰)	δ^{18}O (‰)	δ^2H (‰)	δ^{18}O (‰)	δ^2H (‰)
Burro Burro River	−2.7	−10.1	−7.1	−43.4	–	–	–	–
	−2.7	−9.7	−6.8	−41.5	–	–	–	–
	−2.5	−9.3	−7.6	−47.0	–	–	–	–
	−3.0	−12.4	−3.0	−11.9	–	–	–	–
Tiger Creek	−3.9	−19.8	−4.9	−27.0	−4.3	−19.3	−4.4	−20.8
	−2.7	−10.5	−4.9	−26.5	−3.9	−17.0	−4.5	−21.3
	−3.5	−16.7	−4.9	−26.3	−4.3	−19.1	−4.3	−20.9
	−2.1	−5.9	−5.4	−29.8	−4.8	−23.3	−4.7	−23.0
Blackwater Creek	−2.7	−10.1	−4.9	−25.5	−4.0	−19.5	−4.5	−22.8
	−2.6	−9.5	−4.9	−25.6	−4.0	−19.2	−4.5	−22.6
	−2.6	−9.4	−4.6	−25.5	−4.1	−19.0	−4.4	−22.2
	−2.1	−6.8	−4.8	−25.1	−4.1	−19.3	−4.6	−22.6

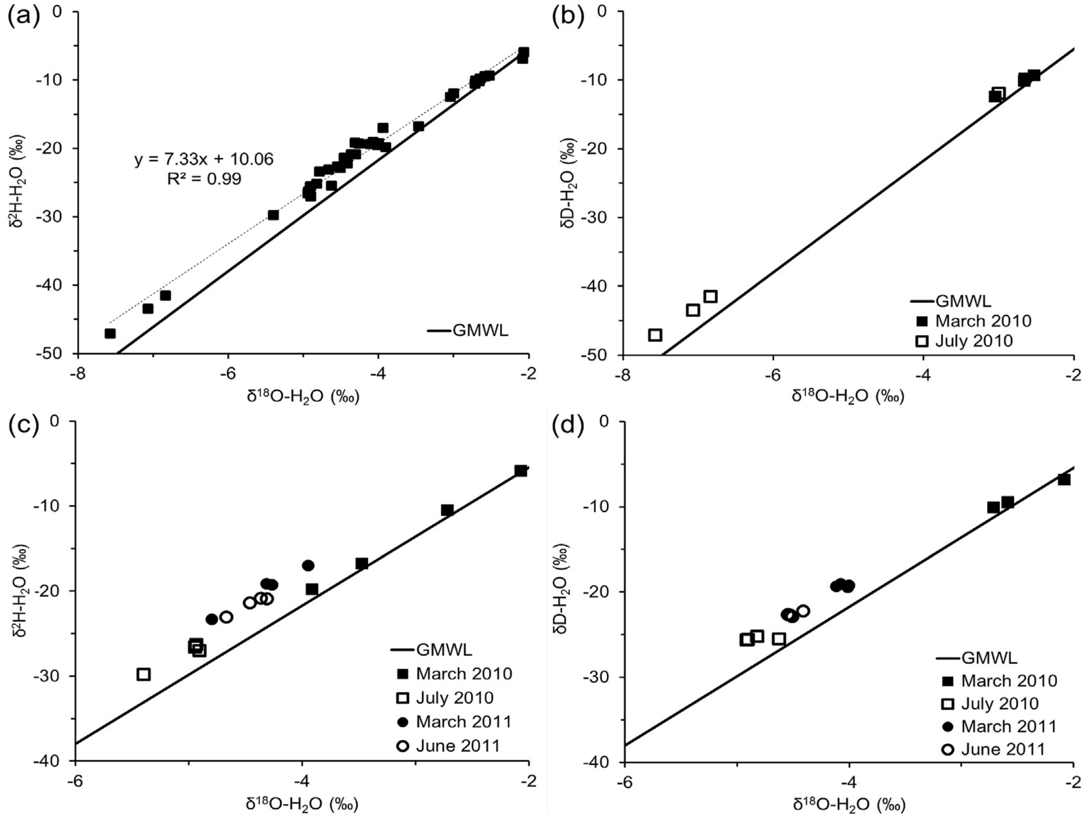

Fig. 4. δ^2H and δ^{18}O values of water plotted against the global meteoric water line (GMWL) of: (a) all river water samples, (b) Burro Burro River 2010, (c) Tiger Creek 2010–2011, (d) Blackwater Creek 2010–2011.

July, with the exception of one sample located at the southern extent of the sampling transect ($\delta^2H = -11.9‰$ and $\delta^{18}O = -3‰$), a decrease in the δ^2H and δ^{18}O values in downstream samples is observed with ranges of δ^2H from −47 to −41.5‰ and δ^{18}O of −7.6 to −6.8‰ (Fig. 4b).

The focus catchments display a similar isotopic pattern from March to July 2010 as observed for the Burro Burro. However, isotopic differences between March (relatively wet month in the dry season) and June (relatively dry month following a wet period) 2011 are not as distinct, with data points more clustered (Fig. 4c and d). The June/July results of Blackwater Creek catchment (Fig. 4d) in both 2010 and 2011 are relatively constant between years and clustered (within 3‰ δ^2H and 0.5‰ δ^{18}O ranges). The ranges of values for δ^2H and δ^{18}O from samples collected in 2010 and 2011 are higher in March (up to 19.0 and 2‰ respectively) compared with June/July. The Tiger Creek 'managed' catchment results (Fig. 4c)

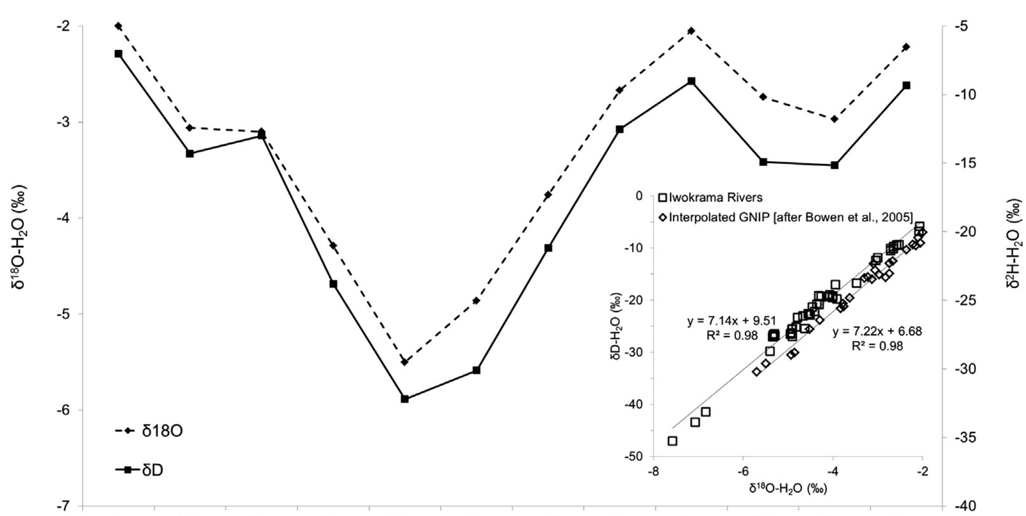

Fig. 5. Interpolated annual isotopic distribution of δ^2H and δ^{18}O values of rainfall for the Iwokrama region with insert of interpolated rainfall isotope values compared against riverine water isotopes collected from 2010 to 2011(after Bowen et al., 2005).

have a similar isotopic pattern to the Blackwater Creek pristine catchment in June/July of 2010 and 2011. However, a wider scattering of the Tiger Creek data along the GMWL compared with the Blackwater Creek data is observed in the March results of both years with the greatest range seen in 2010 (δ^2H: −19.8 to −5.9‰ and δ^{18}O: −3.9 to −2.1‰).

4. Discussion

4.1. Precipitation patterns observed across the forest and savannah of central Guyana compared with TRMM and ERA-Interim models (2009–2011)

Our new climate records from central Guyana are the first published data from this understudied area. A distinct seasonal pattern in rainfall was observed in the forest of Iwokrama between 2009 and 2011, with the peak wet season occurring between May and August and the peak dry season starting in late August. Our field data further show that the secondary wet season that normally occurs around November was more variable, with March being particularly wet in two of the three years (Table 1). Rainfall records from the savannah-rainforest boundary show similar amounts of total monthly rainfall compared with the rainforest, although dry season totals are more variable. There are only small differences in the monthly totals of precipitation between the forest and savannah, indicating that the properties of the air masses crossing the region are not significantly modified by the change in land cover across the spatial scale considered here. The three years of data capture large inter-annual variability. An anomalous southerly shift of the ITCZ, caused by intensification of the tropical Atlantic latitudinal Sea Surface Temperatures (SST) and not ENSO, has been identified as the cause of the May–June 2009 Amazonian floods (Marengo et al., 2012) where rainfall was reduced in Guyana. Conversely, the anomalous migration of the ITCZ to the north in March–May 2010 caused the 2010 central Amazonian drought (Lewis et al., 2011; Marengo et al., 2011), and is also linked with the prolonged wet season in Guyana during these months. The anomalous migrations of the ITCZ were not related to El Nino Southern Oscillation (ENSO), the largest cause of climate variability in the tropics, although ENSO events did occur over our period of study. Over South America, El Nino events cause a southwards shift of the ITCZ whilst La Nina events cause a northward shift (Vera et al., 2006). It has been established that north–east Amazonia has one of the most consistent ENSO-precipitation relationships (Mason and Goddard, 2001; Ropelewski and Halpert, 1987). Along the Guyana coast, ENSO strongly affects rainfall amount, particularly during the secondary wet season (November–January) and secondary dry season (February to April), with El Nino events bringing drought and La Nina events bringing wetter than normal conditions (Wardlaw et al., 2007). This is also the case in north-eastern Brazil and Colombia (Hoyos et al., 2013) in contrast to other Amazonian regions further south which show only weak positive correlations with ENSO manifested as increased rainfall during El Nino (Ronchail et al., 2002). In 2009, relatively mild La Nina conditions lasted until April (http://www.cpc.ncep.noaa.gov/products/analysis_monitoring/ensostuff/ensoyears.shtml, accessed January 2014) causing no discernible impact on rainfall at our study site. This period was followed by ENSO neutral conditions along with the anomalous southerly shift of the ITCZ as described above, causing rainfall levels to be anomalously low. June 2009 brought El Nino conditions, culminating in November 2009 and lasting into February 2010 but rainfall levels remained low. The second anomalous shift of the ITCZ towards the north occurred during March–May and had a large impact, making conditions very wet. From June 2010 until May 2011 strong (intense and of long duration, see Hoyos et al., 2013) La Nina conditions prevailed. A further, but milder La Nina episode occurred between August 2011 and April 2012. Although it is difficult to ascertain the impacts of ENSO on precipitation in central Guyana based on three years of data, the anomalous shifts in the ITCZ appear to have a more pronounced impact on rainfall than ENSO.

The point-scale seasonal pattern of rainfall observed in the forest is broadly consistent with results from grid-scale TRMM and reanalysis data for both ERA-Interim (this study) and ERA-40 (Bovolo et al., 2012). However, the actual amounts of precipitation are greatly underestimated in the peak wet season (both datasets) and overestimated in the dry season (ERA-Interim). ERA-Interim uses temperature, humidity and radiance data to forecast precipitation, which is therefore only indirectly constrained by observations (Dee and Uppala, 2009; Dee et al., 2011; Simmons et al., 2010). In the Amazonia and Guiana region, approximations used in the model's representation of moist processes are not well constrained because of relatively few observations. Consequently, this causes difficulty in modelling convection at coarse spatial scales (Kendon et al., 2012) and affects the quality and consistency of the modelled hydrological cycle (Dee et al., 2011). This is also a problem for Global Climate Models (GCMs), as they tend to depict a relatively weak ITCZ that extends southwards of its observed position, resulting in poor matches with observed precipitation in tropical regions (IPCC, 2007). This makes determining forest vulnerability of Amazonia and the Guiana Shield to climate change difficult (IPCC, 2007). TRMM monthly gauge adjusted satellite estimates at a fine grid-scale resolution are generally better at estimating rainfall, although again rainfall is underestimated in the wet-season at our sites. Given that TRMM data is based on satellite observations that are calibrated with available ground observations it should provide a more realistic precipitation estimate than reanalysis data. Previous studies (de Angelis et al., 2004; Franchito et al., 2009) focussing specifically on the "precipitation radar" component of TRMM found that the satellite data product captures important characteristics of rainfall over the Amazon, but rainfall regimes in less humid climates were less well represented. For combined (multi-sensor) rainfall products in an earlier version (v5) of TRMM, Adler et al. (2000) found a dry bias compared to the Global Precipitation Climatology Project (GPCP) dataset. The TRMM family of spatial precipitation data products was designed primarily to study the convective precipitation dominant in the tropics and sub-tropics. The incorporation of imagery from geostationary satellites (e.g. GOES) to estimate rates of precipitation from observations of cloud top temperatures is particularly suited to convective precipitation rather than orographic and (large-scale) stratiform precipitation. Nevertheless, the less frequent rates of observation (overpass/revisit frequency) of the passive microwave and space-borne precipitation radar used to calibrate the continuous precipitation estimates from geostationary imagery do limit the coherence/consistency of the multi-sensor approach to remote sensing-derived precipitation estimates (Clarke et al., 2011; Collischonn et al., 2008; Dias De Paiva et al., 2011; Dias De Paiva et al., 2011).

4.2. Residence times of water within the Burro Burro catchment

The peak wet and dry conditions of the region from 2010 to 2011 are captured in the δ^2H and δ^{18}O records of river water (Fig. 4) with the most distinct differences between the extreme dry and wet seasons of 2010. The riverine signatures show a notable seasonal isotopic separation that is broadly consistent with the rainfall pattern modelled for the Iwokrama region using the interpolated GNIP datasets by Bowen et al. (2005) (Fig. 6). TRMM images confirm that the spatial positioning of the ITCZ was likely to be responsible

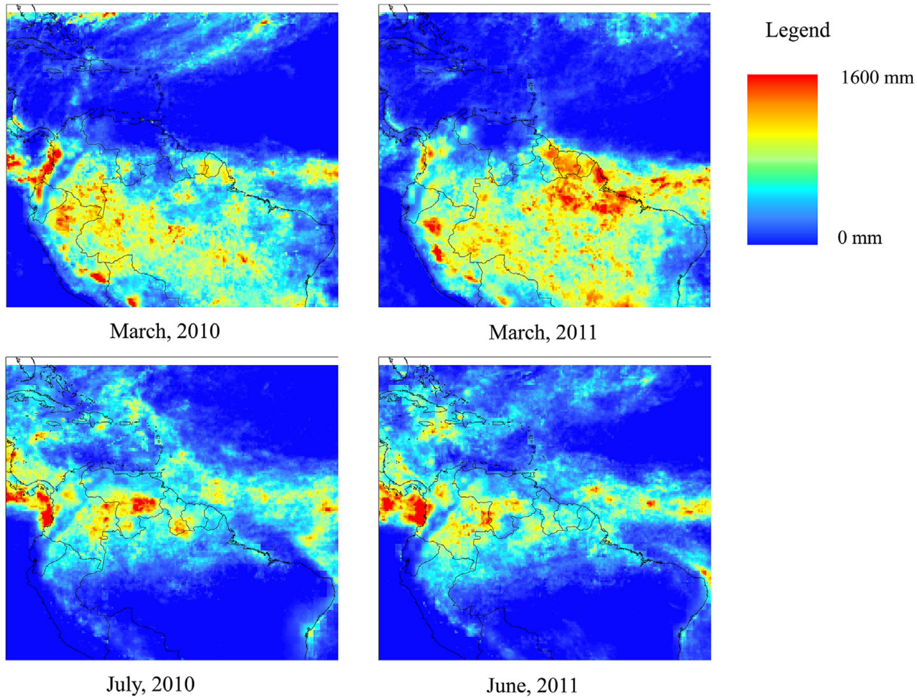

Fig. 6. TRMM images extracted for northern South America from March and July, 2010 and March and June 2011 coinciding with river δ^2H and $\delta^{18}O$ isotope datasets. (For interpretation of the references to colour in this figure legend, the reader is referred to the web version of this article.)

for the isotopically lighter water received by river catchments during the peak wet season (Fig. 6).

Although the river δ^2H and $\delta^{18}O$ datasets are much more variable, this is probably a result of localised effects such as evaporation and a mixing of surficial runoff and baseflow waters. Given the observed seasonal pattern in riverine δ^2H and $\delta^{18}O$ signatures, it suggests that the 'amount effect' (Dansgaard, 1964), which brings isotopically lighter water associated with tropical rains of the ITCZ, is the controlling factor in determining wet season isotopic signatures of river water in the region. This is consistent with other studies from Amazonia (Martinelli et al., 1996; Matsui et al., 1983; Rozanski and Araguás-Araguás, 1995; Salati et al., 1979). A notable exception exists for the uppermost section of the Burro Burro River during the wet season of 2010 (close to the savannah-rainforest transition) that exhibits a similar isotopic signature to the dry season (upper right hollow square in Fig. 4a). This suggests that the rivers draining the upper catchment of the Burro Burro River were not influenced by the ITCZ rains from the north at this time, which is difficult to discern from TRMM datasets alone.

At the small scale, there are no observed differences in δ^2H and $\delta^{18}O$ values between Blackwater and Tiger Creek catchments, suggesting that there is little observable variation in the hydrological cycle from RIL practices (for example, due to evaporation changes as a result of RIL practices). Interestingly, given that the same rainfall totals are recorded in the forest for March and June 2011, there is a notable difference of the δ^2H and $\delta^{18}O$ values in the small scale river catchments. This suggests that differences in the riverine isotopic signatures may capture the preceding hydrological conditions, as would be expected. If so, this time-lag in the hydrological system implies that even at the small-scale there is evidence of a residence time or 'hydrological memory' of precipitation, which may be a month or longer. Further analysis of the hydrological data at higher time resolution will be carried out to investigate this in more detail. This result demonstrates that sensitivity to climatic influences can be detected at the headwater scale, which may not be evident in larger scale catchment studies.

5. Conclusion

We present new data on rainfall, stream flow, and isotopic composition of headwater catchments in central Guyana. The data provide the first field results showing local hydro-climatic behaviour within the Guiana Shield region of northern Amazonia during the period from 2009 to 2011, when anomalous shifts in the ITCZ created exceptionally dry and wet periods during 2010 and 2011 respectively, in contrast to the floods and droughts experienced in the Amazon basin during the same period.

Comparison of these new results with data from TRMM and ERA-Interim global models of precipitation and climate show that the pattern of seasonality (occurrence and timing of wet and dry seasons) is broadly represented by these models, supporting the findings of a previous study using the ERA-40 model (Bovolo et al., 2012). However, monthly precipitation totals are not well characterized by either of these models, with the TRMM and ERA-Interim models underestimating total monthly rainfall by up to 50% and 72% respectively during the wet seasons. The TRMM dataset is generally better at characterising the main dry season from September to December but the ERA-Interim model can overestimate precipitation during the dry season by up to 175%. Although local effects, including topographical variability at the sub-grid scale and the random nature of localised convective storms, may account for some discrepancies, there appear to be systematic biases in the modelled data.

The first new records of river discharge and isotopic geochemistry within headwater catchments in the forest reflect the rainfall patterns of the area, with the $\delta^2H/\delta^{18}O$ isotopic values of the river being broadly consistent with the GNIP rainfall interpolation model (Bowen et al., 2005). The position of the Inter-Tropical Convergence Zone (ITCZ) is shown to influence the isotopic composition of river water, with isotopically lighter water derived from the tropical rainfall of the ITCZ dominating during the wet season.

This dataset from central Guyana provides new field hydro-climate observations in a data-scarce region which may become increasingly important as one of the remaining extensive areas of intact tropical forest of Amazonia, and which may also play a critical regional role in transferring moisture from the Caribbean to the interior of South America. Our comparison of field data against global models of rainfall and geochemistry highlight the existing uncertainties of modelled data that should be taken into account if used for the interpretation of hydrological cycling within large river systems, such as Amazonia. Accurately representing the dynamics of headwater catchments using model data, constrained by field observations, and understanding how this relates to the regional scale is crucial for characterising and quantifying the role of large river systems in continental scale hydrological and biogeochemical cycling. Small headwaters typically comprise by far the largest area of the river catchment and they are the most responsive to climate change, particularly during short term weather events and land use changes superimposed on longer term fluctuations in seasonality. Combining point and local scale data from field observations with regional and global scale model data is a critical step forward to achieve a more integrated and better-calibrated understanding of climate–hydrology interactions in Amazonia.

Acknowledgements

This research was supported by Inter-American Development Bank (IADB) Grant ATN/MC-11548-GY, project GY-T1069-Measurement of Climate Change Impacts and Eco-System Services at Iwokrama. RP acknowledges support from NERC grant NE/H525254/1, TW acknowledges support from the Royal Society Wolfson Research Merit Award, CIB also acknowledges support from the IADB. We thank the whole Iwokrama staff and support team, specifically Angela Franklin–Lewis (Monitoring Manger), and all the rangers, especially Floria Francis, Glenny King, Russian Dorrick for field support, and Ken Rodney, forestry manager. We also thank Robert Posey and Jurian Hoogewerff for help with stable hydrogen and oxygen isotope measurements.

References

Adler, R.F., Huffman, G.J., Bolvin, D.T., Curtis, S., Nelkin, E.J., 2000. Tropical rainfall distributions determined using TRMM combined with other satellite and rain gauge information. J. Appl. Meteorol. 39, 2007–2023. http://dx.doi.org/10.1175/1520-0450(2001)040<2007:TRDDUT>2.0.CO;2.

Adler, R.F., Huffman, G.J., Chang, A., Ferraro, R., Xie, P.P., Janowiak, J., Rudolf, B., Schneider, U., Curtis, S., Bolvin, D., Gruber, A., Susskind, J., Arkin, P., Nelkin, E., 2003. The version-2 global precipitation climatology project (GPCP) monthly precipitation analysis (1979-present). J. Hydrometeorol. 4, 1147–1167. http://dx.doi.org/10.1175/1525-7541(2003)004<1147:tvgpcp>2.0.co;2.

Araguas-Araguas, L., Froehlich, K., Rozanski, K., 2000. Deuterium and oxygen-18 isotope composition of precipitation and atmospheric moisture. Hydrol. Process. 14, 1341–1355. http://dx.doi.org/10.1002/1099–1085(20000615)14:8<1341::aid-hyp983>3.0.co;2-z.

Batistella, M., Artaxo, P., Nobre, C., Bustamante, M., Luizao, F., 2009. Results from LBA and a vision for future amazonian research. In: Keller, M., Bustamante, M., Gash, J., Dias, P.S. (Eds.), Amazonia and Global Change. Amer Geophysical Union, 2000 Florida Ave Nw, Washington, Dc 20009 USA.

Battin, T.J., 1998. Dissolved organic matter and its optical properties in a blackwater tributary of the upper Orinoco river, Venezuela. Org. Geochem. 28, 561–569. http://dx.doi.org/10.1016/s0146-6380(98)00028-x.

Betts, A.K., Köhler, M., Zhang, Y., 2009. Comparison of river basin hydrometeorology in ERA-interim and ERA-40 reanalyses with observations. J. Geophys. Res. Atmos. 114. http://dx.doi.org/10.1029/2008JD010761.

Bohnke, R., Geyer, S., Kowski, P., 2002. Using environmental isotopes H-2 and O-18 for identification of infiltration processes in floodplain ecosystems of the river Elbe. Isot. Environ. Health Stud. 38, 1–13. http://dx.doi.org/10.1080/10256010208033304.

Booth, B.B.B., Dunstone, N.J., Halloran, P.R., Andrews, T., Bellouin, N., 2012. Aerosols implicated as a prime driver of twentieth-century North Atlantic climate variability. Nature 484, 228–232.

Bovolo, C.I., Pereira, R., Parkin, G., Kilsby, C., Wagner, T., 2012. Fine-scale regional climate patterns in the Guianas, tropical South America, based on observations and reanalysis data. Int. J. Climatol. 32, 1665–1689. http://dx.doi.org/10.1002/joc.2387.

Bowen, G.J., Revenaugh, J., 2003. Interpolating the isotopic composition of modern meteoric precipitation. Water Resour. Res. 39. http://dx.doi.org/10.1029/2003wr002086.

Bowen, G.J., Wassenaar, L.I., Hobson, K.A., 2005. Global application of stable hydrogen and oxygen isotopes to wildlife forensics. Oecologia 143, 337–348. http://dx.doi.org/10.1007/s00442-004-1813-y.

Chen, M., Shi, W., Xie, P., Silva, V.B.S., Kousky, V.E., Higgins, R.W., Janowiak, J.E., 2008. Assessing objective techniques for gauge-based analyses of global daily precipitation. J. Geophys. Res. Atmos. 113. http://dx.doi.org/10.1029/2007jd009132.

Clark, I., Fritz, P., 1997. Environmental Isotopes in Hydrogeology. Lewis Publishers, New York.

Clarke, R.T., Buarque, D.C., de Paiva, R.C.D., Collischonn, W., 2011. Issues of spatial correlation arising from the use of TRMM rainfall estimates in the Brazilian Amazon. Water Resour. Res. 47, W05539. http://dx.doi.org/10.1029/2010wr010334.

Collischonn, B., Collischonn, W., Tucci, C.E.M., 2008. Daily hydrological modeling in the Amazon basin using TRMM rainfall estimates. J. Hydrol. 360, 207–216. http://dx.doi.org/10.1016/j.jhydrol.2008.07.032.

Craig, H., 1961. Standard for reporting concentrations of deuterium and oxygen-18 in natural waters. Science 133, 1833–1834. http://dx.doi.org/10.1126/science.133.3467.1833.

Dai, A. and Trenberth, K. E., 2002. Estimates of freshwater discharge from continents: latitudinal and seasonal variations. J. Hydrometeorol. 3, 660-687. DOI: 10.1175/1525-7541(2002)003<0660:eofdfc>2.0.co;2.

Dansgaard, W., 1964. Stable isotopes in precipitation. Tellus 16, 436–468. http://dx.doi.org/10.1111/j.2153-3490.1964.tb00181.x.

Dawson, T.E., Simonin, K.A., 2011. The roles of stable isotopes in Forest hydrology and Biogeochemistry. In: Levia, Delphis F., Carlyle-Moses, Darryl, Tanaka, Tadashi (Eds.), Forest Hydrology and Biogeochemistry: Synthesis of Past Research and Future Directions.

de Angelis, C.F., McGregor, G.R., Kidd, C., 2004. A 3 year climatology of rainfall characteristics over tropical and subtropical South America based on tropical rainfall measuring mission precipitation radar data. Int. J. Climatol. 24, 385–399. http://dx.doi.org/10.1002/joc.998.

Dee, D.P., Uppala, S., 2009. Variational bias correction of satellite radiance data in the ERA-Interim reanalysis. Q. J. Royal Meteorol. Soc. 135, 1830–1841. http://dx.doi.org/10.1002/qj.493.

Dee, D.P., Uppala, S.M., Simmons, A.J., Berrisford, P., Poli, P., Kobayashi, S., Andrae, U., Balmaseda, M.A., Balsamo, G., Bauer, P., Bechtold, P., Beljaars, A.C.M., van de Berg, L., Bidlot, J., Bormann, N., Delsol, C., Dragani, R., Fuentes, M., Geer, A.J., Haimberger, L., Healy, S.B., Hersbach, H., Holm, E.V., Isaksen, L., Kallberg, P., Kohler, M., Matricardi, M., McNally, A.P., Monge-Sanz, B.M., Morcrette, J.J., Park, B.K., Peubey, C., de Rosnay, P., Tavolato, C., Thepaut, J.N., Vitart, F., 2011. The ERA-interim reanalysis: configuration and performance of the data assimilation system. Q. J. Royal Meteorol. Soc. 137, 553–597. http://dx.doi.org/10.1002/qj.828.

Dias De Paiva, R.C., Buarque, D.C., Collischonn, W., Sorribas, M.S., Allasia, D.G.P., Mendes, C.A.B., Tucci, C.E.M., Bonnet, M.-P., 2011. Using TRMM rainfall estimates in hydrological and hydrodynamic modelling of the Amazon Basin. In: Hafeez, M., VanDeGiesen, N., Bardsley, E., Seyler, F., Pail, R., Taniguchi, M. (Eds.), Grace, Remote Sensing and Ground-based Methods in Multi-scale Hydrology.

Eltahir, E.A.B., Bras, R.L., 1994. Precipitation recycling in the Amazon basin. Q. J. Royal Meteorol. Soc. 120, 861–880. http://dx.doi.org/10.1002/qj.49712051806.

Feng, X., Faiia, A.M., Posmentier, E.S., 2009. Seasonality of isotopes in precipitation: a global perspective. J. Geophys. Res. Atmos. 114. http://dx.doi.org/10.1029/2008jd011279.

Franchito, S.H., Rao, V.B., Vasques, A.C., Santo, C.M.E., Conforte, J.C., 2009. Validation of TRMM precipitation radar monthly rainfall estimates over Brazil. J. Geophys. Res. Atmos. 114. http://dx.doi.org/10.1029/2007JD009580.

Fricke, H.C., O'Neil, J.R., 1999. The correlation between O-18/O-16 ratios of meteoric water and surface temperature: its use in investigating terrestrial climate change over geologic time. Earth Planet. Sci. Lett. 170, 181–196. http://dx.doi.org/10.1016/s0012-821x(99)00105-3.

Gat, J.R., 2004. The use of Environmental Isotopes of Water in Catchment Studies.

Gond, V., Freycon, V., Molino, J.-F., Brunaux, O., Ingrassia, F., Joubert, P., Pekel, J.-F., Prevost, M.-F., Thierron, V., Trombe, P.-J., Sabatier, D., 2011. Broad-scale spatial pattern of forest landscape types in the Guiana Shield. Int. J. Appl. Earth Observation Geoinf. 13, 357–367. http://dx.doi.org/10.1016/j.jag.2011.01.004.

Gonfiantini, R., Roche, M.A., Olivry, J.C., Fontes, J.C., Zuppi, G.M., 2001. The altitude effect on the isotopic composition of tropical rains. Chem. Geol. 181, 147–167. http://dx.doi.org/10.1016/s0009-2541(01)00279-0.

Hammond, D.S., 2005. Tropical Forests of the Guiana Shield: Ancient Forests in a Modern World. CAB International.

Hawkes, M.D., Wall, J.R.D., 1993. The Commonwealth and Government of Guyana Rain Forest Programme, Phase I, Site Resource Survey. Main Report. Natural Resources Institute, Chatham, UK.

Henderson-Sellers, A., McGuffie, K., Zhang, H., 2002. Stable isotopes as validation tools for global climate model predictions of the impact of Amazonian deforestation. J. Clim. 15, 2664–2677. http://dx.doi.org/10.1175/1520-0442(2002)015<2664:siavtf>2.0.co;2.

Hoyos, N., Escobar, J., Restrepo, J.C., Arango, A.M., Ortiz, J.C., 2013. Impact of the 2010–2011 La Nina phenomenon in Colombia, South America: the human toll of an extreme weather event. Appl. Geogr. 39, 16–25. http://dx.doi.org/10.1016/j.apgeog.2012.11.018.

Huffman, G.J., Adler, R.F., Bolvin, D.T., Gu, G.J., Nelkin, E.J., Bowman, K.P., Hong, Y., Stocker, E.F., Wolff, D.B., 2007. The TRMM multisatellite precipitation analysis

(TMPA): quasi-global, multiyear, combined-sensor precipitation estimates at fine scales. J. Hydrometeorol. 8, 38–55. http://dx.doi.org/10.1175/jhm560.1.

IPCC, 2007. Climate change 2007: the physical science basis. In: Solomon, S., Qin, D., Manning, M., Chen, Z., Marquis, M., Averyt, K.B., Tignor, M., Miller, H.L. (Eds.), Contribution of Working Group 1 to the Fourth Assessment Report of the Intergovernmental Panel on Climate Change. Cambridge University Press, Cambridge, United Kingdom, New York, NY, USA, 996 pp. Chapter 11 (Regional Climate projections): Section 11.6 (South and Central America).

Kendon, E.J., Roberts, N.M., Senior, C.A., Roberts, M.J., 2012. Realism of rainfall in a very high-resolution regional climate model. J. Clim. 25, 5791–5806. http://dx.doi.org/10.1175/JCLI-D-11-00562.1.

Laraque, A., Moquet, J.-S., Alkattan, R., Steiger, J., Mora, A., Adèle, G., Castellanos, B., Lagane, C., Lopez, J.L., Perez, J., Rodriguez, M., Rosales, J., 2013. Seasonal variability of total dissolved fluxes and origin of major dissolved elements within a large tropical river: the Orinoco, Venezuela. J. South Am. Earth Sci. 44, 4–17. http://dx.doi.org/10.1016/j.jsames.2012.12.011.

Lewis, S.L., Brando, P.M., Phillips, O.L., van der Heijden, G.M., Nepstad, D., 2011. The 2010 amazon drought. Science 331, 554. http://dx.doi.org/10.1126/science.1200807.

Li, X.-H., Zhang, Q., Xu, C.-Y., 2012. Suitability of the TRMM satellite rainfalls in driving a distributed hydrological model for water balance computations in Xinjiang catchment, Poyang lake basin. J. Hydrol. 426–427, 28–38. http://dx.doi.org/10.1016/j.jhydrol.2012.01.013.

Macpherson, A.J., Schulze, M.D., Carter, D.R., Vidal, E., 2010. A model for comparing reduced impact logging with conventional logging for an Eastern Amazonian Forest. For. Ecol. Manag. 260, 2002–2011. http://dx.doi.org/10.1016/j.foreco.2010.08.050.

Macpherson, A.J., Carter, D.R., Schulze, M.D., Vidal, E., Lentini, M.W., 2012. The sustainability of timber production from Eastern Amazonian forests. Land Use Pol. 29, 339–350. http://dx.doi.org/10.1016/j.landusepol.2011.07.004.

Marengo, J.A., 2009. Long-term trends and cycles in the hydrometeorology of the Amazon basin since the late 1920s. Hydrol. Process. 23, 3236–3244. http://dx.doi.org/10.1002/hyp.7396.

Marengo, J.A., Tomasella, J., Alves, L.M., Soares, W.R., Rodriguez, D.A., 2011. The drought of 2010 in the context of historical droughts in the Amazon region. Geophys. Res. Lett. 38. http://dx.doi.org/10.1029/2011gl047436.

Marengo, J., Tomasella, J., Soares, W., Alves, L., Nobre, C., 2012. Extreme climatic events in the Amazon basin. Theor. Appl. Climatol. 107, 73–85. http://dx.doi.org/10.1007/s00704-011-0465-1.

Martinelli, L.A., Victoria, R.L., Sternberg, L.S.L., Ribeiro, A., Moreira, M.Z., 1996. Using stable isotopes to determine sources of evaporated water to the atmosphere in the Amazon basin. J. Hydrol. 183, 191–204. http://dx.doi.org/10.1016/0022-1694(95)02974-5.

Martinez, J.-M., Carretier, S., Santos, R.V., 2013. The hydrology, geochemistry, and dynamics of South American great river systems. J. South Am. Earth Sci. 44, 1–3.

Mason, S.J., Goddard, L., 2001. Probabilistic precipitation anomalies associated with ENSO. Bull. Am. Meteorol. Soc. 82, 619–638. http://dx.doi.org/10.1175/1520-0477(2001)082<0619:ppaawe>2.3.co;2.

Matsui, E., Salati, E., Ribeiro, M.N.G., Reis, C.M., Tancredi, A.C.S.N.F., Gat, J.R., 1983. Precipitation in the central Amazon basin the isotopic composition of rain and atmospheric moisture at Belem and Manaus Brazil. Acta Amaz. 13, 307–370.

Mayorga, E., Aufdenkampe, A.K., Masiello, C.A., Krusche, A.V., Hedges, J.I., Quay, P.D., Richey, J.E., Brown, T.A., 2005. Young organic matter as a source of carbon dioxide outgassing from Amazonian rivers. Nature 436, 538–541. http://dx.doi.org/10.1038/nature03880.

McSweeney, C., New, M., Lizcano, G., Lu, X., 2010. The UNDP climate change Country Profiles improving the accessibility of observed and Projected climate information for studies of climate change in developing Countries. Bull. Am. Meteorol. Soc. 91, 157–166. http://dx.doi.org/10.1175/2009bams2826.1.

Miller, S.D., Goulden, M.L., Hutyra, L.R., Keller, M., Saleska, S.R., Wofsy, S.C., Silva Figueira, A.M., da Rocha, H.R., de Camargo, P.B., 2011. Reduced impact logging minimally alters tropical rainforest carbon and energy exchange. Proc. Natl. Acad. Sci. U S A 108, 19431–19435. http://dx.doi.org/10.1073/pnas.1105068108.

Pereira, R., Bovolo, C.I., Spencer, R.G.M., Hernes, P.J., Tipping, E., Vieth-Hillebrand, A., Pedentchouk, N., Chappell, N.A., Parkin, G., Wagner, T., 2014. Mobilization of optically invisible dissolved organic matter (iDOM) in response to rainstorm events in a tropical forest headwater river, 2013GL058658 Geophys. Res. Lett.. http://dx.doi.org/10.1002/2013gl058658.

Pinard, M.A., Putz, F.E., 1996. Retaining forest biomass by reducing logging damage. Biotropica 28, 278–295. http://dx.doi.org/10.2307/2389193.

Richey, J.E., Hedges, J.I., Devol, A.H., Quay, P.D., Victoria, R., Martinelli, L., Forsberg, B.R., 1990. Biogeochemistry of carbon in the amazon river. Limnol. Oceanogr. 35, 352–371.

Richey, J.E., Krusche, A.V., Johnson, M.S., da Cunha, H.B., Ballester, M.V., 2011. The role of rivers in the regional carbon balance. In: Keller, M., Bustamante, M., Gash, J., Dias, P.S. (Eds.), Amazonia and Global Change. Amer Geophysical Union, 2000 Florida Ave Nw, Washington, Dc 20009, USA.

Ronchail, J., Cochonneau, G., Molinier, M., Guyot, J.L., Chaves, A.G.D., Guimaraes, V., de Oliveira, E., 2002. Interannual rainfall variability in the Amazon basin and sea-surface temperatures in the equatorial Pacific and the tropical Atlantic Oceans. Int. J. Climatol. 22, 1663–1686. http://dx.doi.org/10.1002/joc.815.

Ropelewski, C.F., Halpert, M.S., 1987. Global and regional scale precipitation patterns associated with the El-Nino southern oscillation. Mon. Weather Rev. 115, 1606–1626. http://dx.doi.org/10.1175/1520-0493(1987)115<1606:Garspp>2.0.Co;2.

Rozanski, K., Araguás-Araguás, L., 1995. Spatial and temporal variability of stable isotope composition of precipitation over the South American continent. Bull. Inst. Fr. études Andin. 24, 379–390.

Rozanski, K., Araguás-Araguás, L., Gonfiantini, R., 1993. Isotopic Patterns in Modern Global Precipitation, Climate Change in Continental Isotopic Records. AGU, Washington, DC.

Salati, E., Dallolio, A., Matsui, E., Gat, J.R., 1979. Recycling of water in the Amazon basin – isotopic study. Water Resour. Res. 15, 1250–1258. http://dx.doi.org/10.1029/WR015i005p01250.

Saylor, J.E., Mora, A., Horton, B.K., Nie, J., 2009. Controls on the isotopic composition of surface water and precipitation in the Northern Andes, Colombian Eastern Cordillera. Geochim. Cosmochim. Acta 73, 6999–7018. http://dx.doi.org/10.1016/j.gca.2009.08.030.

Shi, W., Higgins, R.W., Yarosh, E., Kousky, V.E., 2000. The Annual Cycle and Variability of Precipitation in Brazil. In: NCEP/Climate Prediction Center Atlas, 9, 25 pp. Available at. http://www.cpc.ncep.noaa.gov/researchpapers/ncepcpcatlas/9/index.html. and from the Climate Prediction Center, World Weather Building, Camp Springs, MD.

Silva, V.B.S., Kousky, V.E., Shi, W., Higgins, R.W., 2007. An improved gridded historical daily precipitation analysis for Brazil. J. Hydrometeorol. 8 (4), 847–861. http://dx.doi.org/10.1175/JHM598.1.

Simmons, A.J., Willett, K.M., Jones, P.D., Thorne, P.W., Dee, D.P., 2010. Low-frequency variations in surface atmospheric humidity, temperature, and precipitation: Inferences from reanalyses and monthly gridded observational data sets. J. Geophys. Res. Atmos. 115. http://dx.doi.org/10.1029/2009jd012442.

Sombroek, W., 2001. Spatial and temporal patterns of Amazon rainfall – consequences for the planning of agricultural occupation and the protection of primary forests. Ambio 30, 388–396. http://dx.doi.org/10.1639/0044-7447(2001)030[0388:satpoa]2.0.co;2.

Speed, M., Tetzlaff, D., Hrachowitz, M., Soulsby, C., 2011. Evolution of the spatial and temporal characteristics of the isotope hydrology of a montane river basin. Hydrol. Sci. J. J. Des. Sci. Hydrol. 56, 426–442. http://dx.doi.org/10.1080/02626667.2011.561208.

Strauch, G., Oyarzun, J., Fiebig-Wittmaack, M., Gonzalez, E., Weise, S.M., 2006. Contributions of the different water sources to the Elqui river runoff (northern Chile) evaluated by H/O isotopes. Isot. Environ. Health Stud. 42, 303–322. http://dx.doi.org/10.1080/10256010600839707.

Sturm, C., Hoffmann, G., Langmann, B., 2007. Simulation of the stable water isotopes in precipitation over South America: comparing regional to global circulation models. J. Clim. 20, 3730–3750. http://dx.doi.org/10.1175/jcli4194.1.

Tardy, Y., Bustillo, V., Roquin, C., Mortatti, J., Victoria, R., 2005. The Amazon. Biogeochemistry applied to river basin management Part I. Hydro-climatology, hydrograph separation, mass transfer balances, stable isotopes, and modelling. Appl. Geochem. 20, 1746–1829. http://dx.doi.org/10.1016/j.apgeochem.2005.06.001.

Tomasella, J., Borma, L.S., Marengo, J.A., Rodriguez, D.A., Cuartas, L.A., Nobre, C.A., Prado, M.C.R., 2011. The droughts of 1996–1997 and 2004–2005 in Amazonia: hydrological response in the river main-stem. Hydrol. Process. 25, 1228–1242. http://dx.doi.org/10.1002/hyp.7889.

Vera, C., Silvestri, G., Liebmann, B., Gonzalez, P., 2006. Climate change scenarios for seasonal precipitation in South America from IPCC-AR4 models. Geophys. Res. Lett. 33. http://dx.doi.org/10.1029/2006gl025759.

Vuille, M., Werner, M., 2005. Stable isotopes in precipitation recording South American summer monsoon and ENSO variability: observations and model results. Clim. Dyn. 25, 401–413. http://dx.doi.org/10.1007/s00382-005-0049-9.

Vuille, M., Bradley, R.S., Werner, M., Healy, R., Keimig, F., 2003. Modeling delta O-18 in precipitation over the tropical Americas: 1. Interannual variability and climatic controls. J. Geophys. Res. Atmos. 108. http://dx.doi.org/10.1029/2001jd002038.

Wardlaw, R., Jaigopaul, D., Rahaman, Z., 2007. Influence of El Nino on rainfall in Guyana and Uganda. Proc. Institution Civ. Eng. Water Manag. 160, 135–143. http://dx.doi.org/10.1680/wama.2007.160.3.135.

Wassenaar, L.I., Athanasopoulos, P., Hendry, M.J., 2011. Isotope hydrology of precipitation, surface and ground waters in the Okanagan Valley, British Columbia, Canada. J. Hydrol. 411, 37–48. http://dx.doi.org/10.1016/j.jhydrol.2011.09.032.

Xie, P., Arkin, P.A., 1997. Global Precipitation: A 17-Year Monthly Analysis Based on Gauge Observations. Satellite Estimates, and Numerical Model Outputs. Bull. Am. Meteorol. Soc. 78, 2539–2558. http://dx.doi.org/10.1175/1520-0477(1997)078<2539:GPAYMA>2.0.CO;2.

Yamashita, Y., Maie, N., Briceno, H., Jaffe, R., 2010. Optical characterization of dissolved organic matter in tropical rivers of the Guayana Shield, Venezuela. Artn G00f10 J. Geophys. Res. Biogeosci. 115. http://dx.doi.org/10.1029/2009jg000987.